Biochemical and Biophysical Research Communications 447 (2014) 184–191

Contents lists available at ScienceDirect

Biochemical and Biophysical Research Communications

journal homepage: www.elsevier.com/locate/ybbrc

mTOR-targeted therapy: Differential perturbation to mitochondrial membrane potential and permeability transition pore plays a role in therapeutic response

Jae Eun Kim [b], Qun He [a], Yaqing Chen [a], Celine Shi [b], Ker Yu [a,b,*]

[a] Department of Pharmacology, Fudan University, School of Pharmacy, Shanghai 201203, China
[b] Oncology Research, Pfizer Pharmaceuticals, Pearl River, NY 10965, USA

ARTICLE INFO

Article history:
Received 19 March 2014
Available online 2 April 2014

Keywords:
mTOR inhibitor
Mitochondria
Anticancer

ABSTRACT

While cancer cell mitochondria mediate actions of many successful chemotherapeutics, little is known about mitochondrial response in mTOR-targeted anticancer therapy. We have studied mitochondrial dynamics in relation to growth suppression employing an allosteric inhibitor rapalog, a highly selective mTOR kinase inhibitor (mTOR-KI) and mTOR-ShRNA. Global targeting of mTOR increased mitochondrial membrane potential ($m\Delta\psi$) and inhibited mitochondrial permeability transition pore (mPTP). Importantly, these mTOR-KI-provoked anti-survival and pro-survival effects were differentially manifested in diverse cancer cells according to intrinsic susceptibility to mTOR-targeting. The most-sensitive cells including those possessing hyperactive PI3K/AKT/mTOR and/or growth factor-dependence (LNCap, MDA361 and MG63) all displayed a dramatic increase in $m\Delta\psi$, whereas the $m\Delta\psi$ increase was not evident in majority of resistant cancer cells. Upon mTOR-KI treatment, the resistant cells including those harboring K-Ras- or B-Raf mutation (MDA231, HT29 and HCT116) all displayed a markedly reduced mPTP opening, which paralleled a sustained AKT-hexokinase 2 (HK2) survival signaling and persistent phosphorylation (inactivation) of GSK3β. Further studies demonstrated that the mTOR-KI-provoked mPTP closure in resistant cells was mediated through an enhanced binding of HK2 to the mitochondrial voltage-dependent anion channel (VDAC), a molecular mechanism known to promote mPTP closure and cell survival. Detaching HK2 from VDAC by an HK2-displacing peptide or methyl jasmonate specifically blocked the mTOR-KI-provoked mPTP closure and potentiated growth suppression in resistant cells. Thus, mTOR-inhibition can exert complex and differential perturbation to mitochondrial dynamics in cancer cells, which likely influence therapeutic outcome of mTOR-targeted therapy.

1. Introduction

The mechanistic target of rapamycin (mTOR) plays a central role in cellular translation, cell growth and energy metabolism [1,2]. In mammals mTOR exists in two multiprotein complexes, mTORC1 and mTORC2. mTORC1 is sensitive to rapamycin, whereas mTORC2 is insensitive to rapamycin in some settings. mTORC1 regulates protein translation by phosphorylating 4E-BP1 and S6K1, whereas mTORC2 phosphorylates several AGC kinases such as AKT, SGK, and PKC-α. mTOR acts as a central regulator of metabolic homeostasis by sensing and integrating nutrient availability and growth factor signals. Previous studies have demonstrated that rapamycin treatment reduced glycolysis and lipid synthesis, and increased lipolysis and lipid oxidation in many tissues [3].

mTOR plays an increasingly important role in mitochondrial dynamics. Rapamycin treatment or knockdown of mTOR in muscle cells in vitro demonstrated a repression of mitochondrial gene expression [4]. The level of mTORC1 correlates with overall mitochondrial function, G_0–G_1 progression of cell cycle and cell differentiation [5–7]. Additional studies demonstrated that mTOR is present in mitochondria and regulates mitochondrial phosphoproteome [5,8].

Much less is known about mTOR function in cancer cell mitochondrial dynamics. More recent studies have suggested that mTORC2-AKT axis mediates growth factor signaling at mitochondria-associated endoplasmic reticulum membranes [9] and subsets of mTORC2-dysregulated cancer cells are more dependent on mitochondria [10]. mTOR binds and regulates the voltage-dependent anion channel (VDAC) proteins [11], which are situated in the outer

* Corresponding author at: Department of Pharmacology, Fudan University, School of Pharmacy, Shanghai 201203, China.
E-mail address: keryu@fudan.edu.cn (K. Yu).

http://dx.doi.org/10.1016/j.bbrc.2014.03.124
0006-291X/

mitochondrial membrane (OMM) and are a key component of the mitochondrial permeability transition pore (mPTP). The mTORC2-AKT also promotes phosphorylation of hexokinase 2 (HK2) and enhances HK2 binding to VDAC thereby enhancing aerobic glycolysis and survival in cancer cells [12].

We previously reported the molecular profile of WYE-132, a highly potent and specific mTOR kinase inhibitor (mTOR-KI) [13]. WYE-132 and related mTOR-KIs globally target mTORC1 and mTORC2 and are mechanistically differentiated from the clinically used rapamycin-like drugs (rapalogs) which partially inhibit mTOR [14]. We found that mTOR-KIs are generally stronger growth inhibitors than rapalogs. Meanwhile, these compounds still elicited rather variable anti-proliferative responses when assayed in cell lines of diverse cancer types. Employing WYE-132, the rapalog CCI-779 and mTOR-targeting shRNA, we have studied novel roles of mTOR in mitochondrial function in diverse cancer cells in relation to antitumor activity. Our results demonstrate that global targeting of mTOR caused both anti-survival and pro-survival mitochondrial responses, which were differentially manifested in diverse cancer cells according to their intrinsic susceptibility to mTOR inhibition.

2. Materials and methods

2.1. Chemicals and shRNA

WYE-132 and CCI-779 were provided by Wyeth Chemistry and purchased from BiochemPartner (Shanghai) for work at Wyeth and Fudan University, respectively. UO126 and cisplatin (BiochemPartner), methyl jasmonate (Sigma), cell-permeable form of HXK2VBD (CalBiochem) were purchased. GIPZ shRNAs of non-targeting and mTOR (Open Biosystems) were validated according to manufacturer's instruction. Cells were infected with viral particles, selected under puromycin for 3–5 days then used in various studies.

2.2. Cell culture and growth assay

A498, LNCap, MDA361, MG63, MDA231, HCT116 and HT29 cells (ATCC) were maintained with standard culture methods using cell culture reagents (GIBCO). Cells were seeded in 96-well plates and treated with inhibitors alone or in combination in triplicates. Cell viability was measured 3 days later by MTS cell titer 96 Aqueous one solution cell proliferation assay (Promega), measured by absorbance at 490 nm.

2.3. Mitochondrial membrane potential ($m\Delta\psi$)

$m\Delta\psi$ was assessed using 5,5′,6,6′-tetrachloro-1,1′,3,3′-tetraethylbenzimidazole carbocyanide iodide (JC-1; Invitrogen). Cells were grown until 90% confluence and treated with inhibitors as indicated. Cells were washed with PBS and incubated at 37 °C for 15 min with 6.5 μM JC-1 in serum-free media in the dark. J-aggregates were monitored using fluorescent microscope.

2.4. mPTP permeability assay

Permeability of mPTP was measured using Image-iT™ mitochondrial transition pore assay kit (Invitrogen). Principle of the assay is described previously [15]. In dye post-loading protocol, cells were treated with inhibitors for 1 h, washed with PBS and incubated with 1 μM calcein AM and 1 mM $CoCl_2$ in the modified HBSS buffer for 15 min at 37 °C. mPTP permeability change was assessed by measuring calcein fluorescence intensity. In dye pre-loading protocol, calcein/$CoCl_2$ pre-loaded cells were treated with inhibitors, and the opening of mPTP was induced by 250 μM ionomycin for 30 min prior to fluorescence intensity measurement.

2.5. O_2 consumption

Cells grown in culture flasks were trypsinized, resuspended in glucose-free DMEM with 10% dialyzed FBS. Cell suspension was aliquoted and inhibitors were added to each aliquot. After 1 h of incubation, cell suspension was measured for O_2 consumption rate as described [13].

2.6. Immunofluorescent staining

A498 cells grown on cover-slips were fixed with 3.7% formaldehyde, blocked with 10% FBS in PBS for 30 min, stained with 2 μg/ml mouse anti-VDAC1 and goat anti-HK2 (Santa Cruz) in blocking buffer for 1 h. The cells were rinsed with PBS, stained with Alexa fluor® 488-conjugated donkey anti-goat IgG or anti-rabbit IgG (Invitrogen) and Alexa fluor® 594-conjugated donkey anti-mouse IgG (Invitrogen) for 30 min at room temperature, rinsed with PBS and mounted in Prolong Antifade (Invitrogen). The cells were observed with a confocal immunofluorescent microscope using a 60× plan objective.

2.7. Immunoprecipitation and immunoblotting

A498 cells were treated with inhibitors for 1 h, lysed in 20 mM HEPES (pH 7.4), 150 mM NaCl, 1 mM EDTA, 0.1% CHAPS, 1 mM DTT and harvested by scraping. Clear lysates were combined with 2 μg of anti-HK2 antibody (CST) and rocked overnight at 4 °C. 15 μl (packed gel) of protein A/G agarose (Pierce) were added and incubated for 1 h. Immunocomplexes were washed 5× with cell lysis buffer, resuspended in 30 μl NuPAGE LDS sample buffer (Invitrogen) followed by immunoblotting. In other experiments cells were seeded in 6- or 12-well plates, treated with inhibitors, washed with PBS and lysed in LDS sample buffer. For mTOR knockdown experiments, puromycin-selected cells were plated and lysed in LDS sample buffer. Primary antibodies of P-AKT(S473), P-AKT(T308), AKT, P-GSK3(S21/9), P-4EBP-1(T70), P-S6K1(T389), HK2, mTOR and cyclin D1 (CST), c-Myc (Santa Cruz), β-actin and GAPDH (Bioworld) were obtained.

3. Results

3.1. mTOR-KI elicits differential responses in growth suppression in diverse cancer lines

Rapalog therapy such as Torisel/CCI-779 is already used clinically for treating renal cell carcinoma (RCC). In proliferation assay of a commonly used RCC A498 line, mTOR-KI WYE-132 elicited a deeper inhibition than CCI-779 in a wide dose range (Fig. 1A) correlating a stronger reduction of cyclin D1 and G_0–G_1 cell cycle progression (not shown). Despite being a stronger inhibitor than the rapalog, WYE-132 elicited rather variable responses when assayed in cell lines of diverse cancer types, which was indicated by both the inhibition concentration 50 (IC_{50}) and inhibition concentration 90 (IC_{90}) values (Fig. 1B). The most sensitive LNCap prostate, MDA361 breast and MG63 osteosarcoma cells were all 90% inhibited with IC_{90} values <0.5 μM, while several resistant lines A498 RCC, MDA231 breast, HCT116 and HT29 colon tumor cells displayed IC_{90} values of 20 μM or higher (Fig. 1B). Immunoblotting analysis with WYE-132-treated MDA361, MG63, HCT116 and HT29 cells showed that both mTORC1 substrate P-S6K(T389) and mTORC2 substrate P-AKT(S473) were potently inhibited in all cell lines, while the growth oncogene c-Myc was only potently

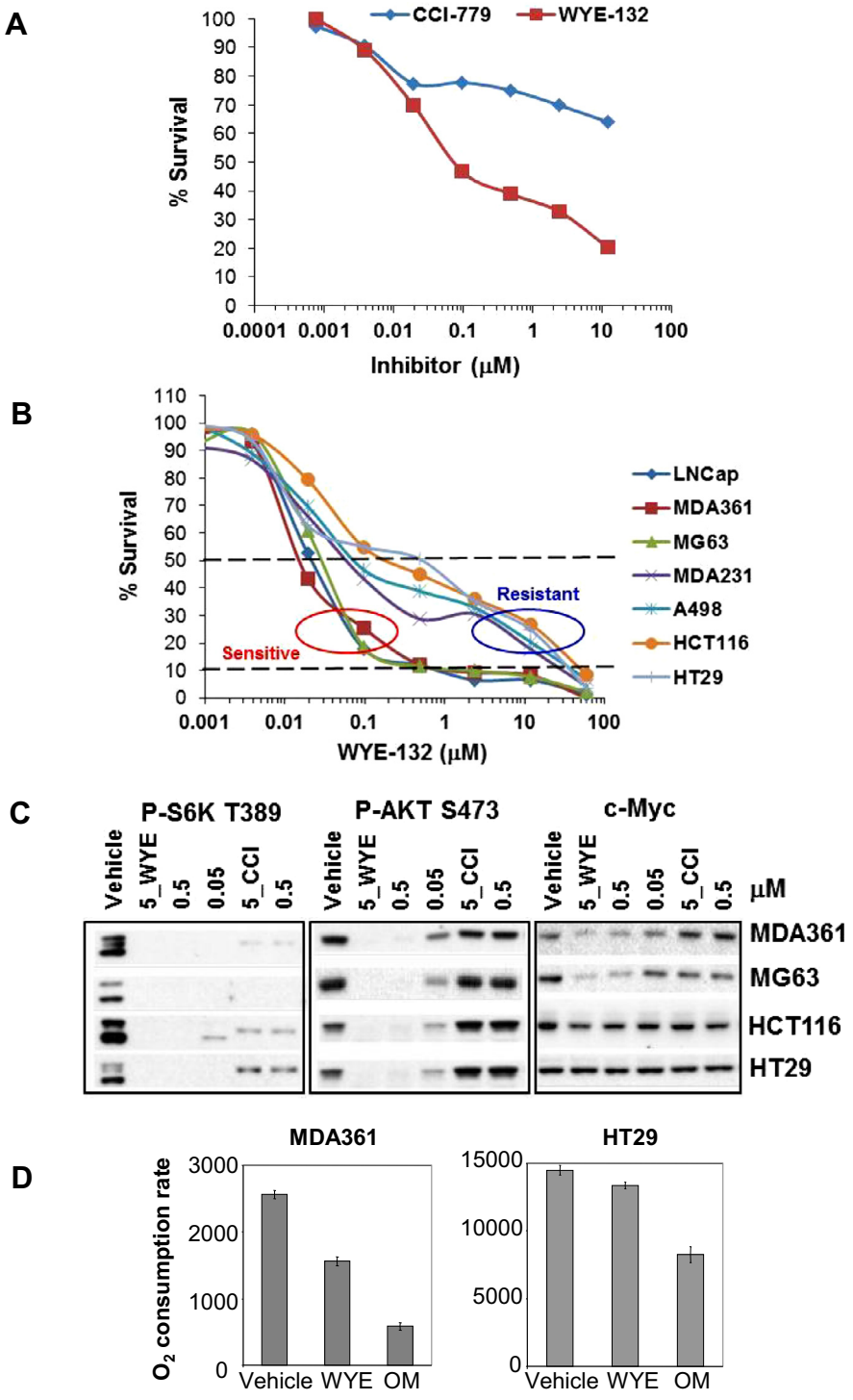

Fig. 1. mTOR-targeting elicits differential responses in growth suppression in diverse cancer lines. (A) Growth inhibition dose curves A498 cells after treatment with various doses of CCI-779 and WYE-132 for 3 days. (B) Growth inhibition dose curves of various cell lines after treatment with various doses of WYE-132 for 3 days. The dashed lines mark 50% and 90% growth inhibition, and the red- and blue circle denote the sensitive- and resistant cell group. (C) MDA361, MG63, HCT116 and HT29 cells were plated in 6-well culture plates, treated with inhibitors for 6 h, then immunoblotted. (D) MDA361 and HT29 were treated with 1 μM WYE-132 (WYE) or oligomycin (OM) for 1 h and O_2 consumption rate was measured for a period of 4 h.

inhibited in sensitive lines MDA361 and MG63 (Fig. 1C). WYE-132 acutely and more substantially reduced oxygen consumption rate in the sensitive MDA361 as compared to the resistant HT29 (Fig. 1D). Therefore, WYE-132 entered into cells and targeted mTORC1- and mTORC2-biomarkers similarly in all cells but elicited quite different antitumor activity in sensitive and resistant tumor cells.

3.2. A massive increase in mitochondrial membrane potential ($m\Delta\psi$) reflects growth inhibition susceptibility to mTOR-inhibition

Having established the variable cellular responses to mTOR-KI, we wished to examine mitochondrial dynamics in relation to growth suppression. We first asked whether WYE-132 or CCI-779 treatment influences mitochondrial energetic status as measured

by the relative membrane potential across the inner membrane of mitochondria (mΔψ). We stained live cells with JC-1 that forms fluorescent J-aggregates when mitochondrial membrane hyperpolarizes. In A498 RCC cells, while 1 μM CCI-779 had little effect, 1 μM WYE-132 caused an occasional formation of J-aggregates in small portion of treated-cells and JC-1-staining was not detected with 30 μM UO126 (MEK inhibition) or cis-platin (Fig. 2A). Significantly, following treatment with 1 μM WYE-132, all of the most-sensitive LNCap, MDA361 and MG63 cells displayed a massive increase in mΔψ as shown by the J-aggregates appeared in nearly all treated population (Fig. 2B). In contrast, similar treatment of the resistant MDA231, HT29 and HCT116 cells with 1 μM WYE-132 showed little increase in mΔψ (Fig. 2B). As the result with A498 cells, treatment of these 6 cell lines with 30 μM UO126 did not induce mΔψ (Fig. 2B).

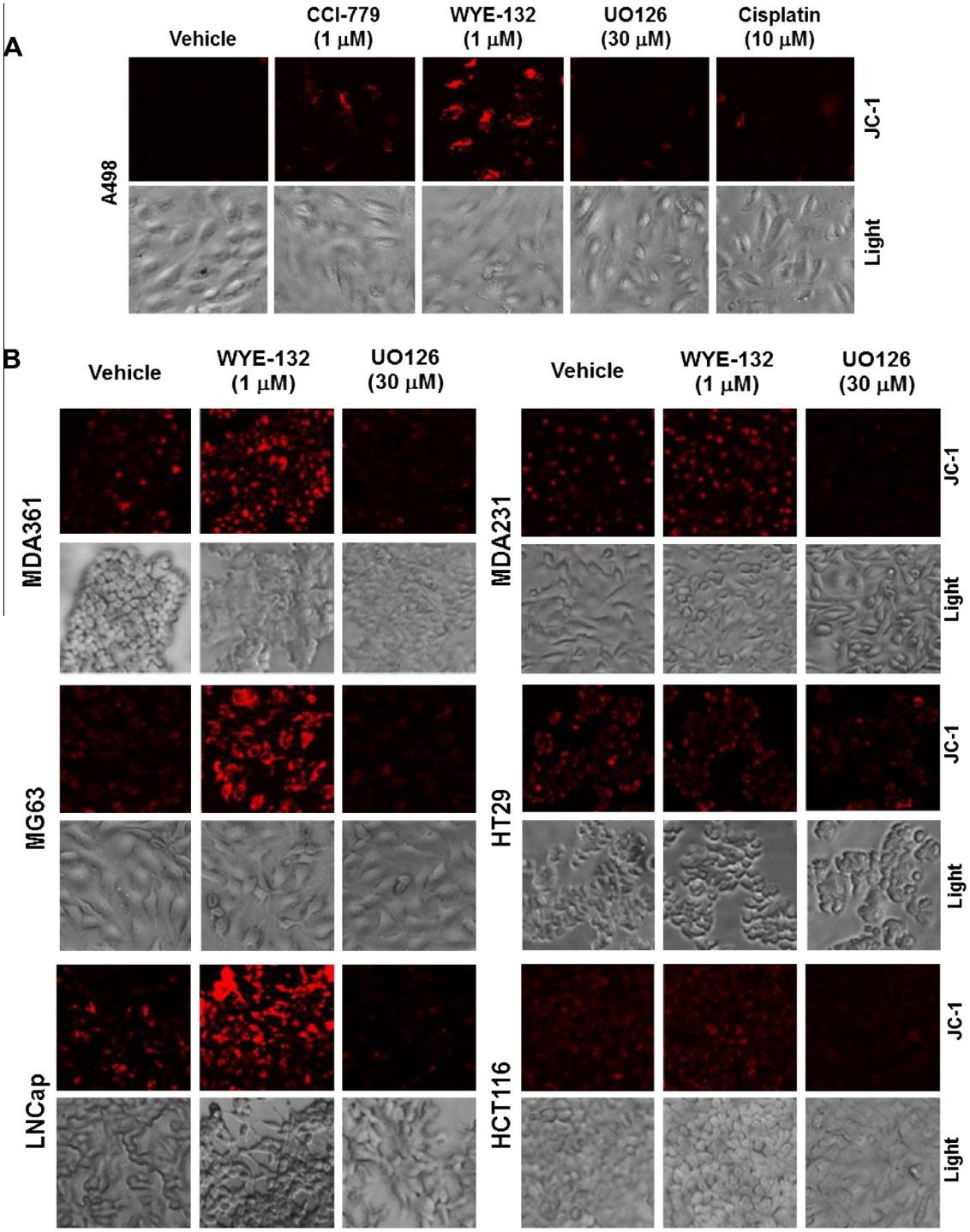

Fig. 2. WYE-132 elicits an increased $\Delta\psi_m$ reflecting growth inhibition susceptibility to mTOR inhibition. (A) A498 cells were plated in 12-well plates, treated with the indicated inhibitors for 16 h. (B) MDA361, MG63, LNCap, MDA231, HT29 and HCT116 cells were similarly plated, treated as indicated for 16 h. The treated cells were stained with JC-1 as described in Section 2 and were taken in light- and fluorescent images.

3.3. mTOR-knockdown leads to a dramatic increase of mΔψ in mTOR-KI-sensitive cells

We next conducted mTOR knockdown via shRNA in 4 representative sensitive and resistant lines. Levels of mTOR were reduced in sh-mTOR-transfected cells (Fig. 3A), which paralleled a deeper growth suppression in MDA361 and MG63 cells compared to that of MDA231 and HT29 cells (Fig. 3B). Remarkably, down-modulation of mTOR selectively increased mΔψ in MDA361 and MG63 but not in MDA231 and HT29 cells (Fig. 3C). In MDA361 and MG63 cells, formation of J-aggregates was detected in nearly 100% of the mTOR-shRNA-expressing cells (Fig. 3C). The results in Figs. 2 and 3 collectively demonstrate that global suppression of mTOR leads to a substantial increase of mΔψ in the mTOR-KI-susceptible cancer cells, which may be mechanistically linked to antitumor efficacy response.

3.4. The mTOR-KI-provoked mPTP closure reflects cellular resistance to mTOR-targeting and involves an enhanced HK2-VDAC association

mPTP opening is often involved in cellular response to chemotherapeutic drugs and apoptosis [16]. We next examined mPTP permeability employing mitochondrial calcein fluorescence after quenching with $CoCl_2$ [15]. Calcein co-loaded with $CoCl_2$ was visualized as compartmented bodies and localized in the mitochondria as confirmed by co-staining with MitoTracker (not shown). In a quantitative plate assay with A498 cells, while CCI-779 had a moderate effect, 0.1 and 1 μM WYE-132 dose dependently inhibited mPTP (higher calcein fluorescence), comparable to that of 10 μM cyclosporine A (CsA), a known blocker of mPTP via targeting cyclophilin D (Cyp-D) of the inner membrane (Fig. 4A, left) [17]. In calcein/$CoCl_2$ pre-loaded A498 cells, ionomycin-induced loss of calcein fluorescence (pore opening) was also significantly inhibited by 100 nM WYE-132 and 10 μM CsA but minimally by 100 nM CCI-779 (Fig. 4A, right). These data indicate that mPTP opening in A498 cells is reduced after mTOR-KI treatment. We next performed calcein/$CoCl_2$ assays in same panel of sensitive and resistant cells. Strikingly, a reduced mPTP opening was most prominently observed ($P < 0.05$) in HT29, HCT116 and MDA231, whereas MDA361 and MG63 showed modest changes (Fig. 4B). Since mPTP closure is previously linked to AKT survival pathway via activation of HK2 [18,19] and inactivating-phosphorylation of GSK3β [20,21], AKT signaling may respond differently in these cells. After 24 h treatment of MDA361, MG63, HT29 and HCT116 cells with WYE-132, while the mTORC2 biomarker P-AKT(S473) was invariably inhibited, there was a highly significant elevation in P-AKT(T308) in HT29 and HCT116 but not in MDA361 and MG63 cells (Fig. 4C). Likewise, inactivating P-GSK3β(S9/21) was significantly reduced in MDA361 and MG63 but not in HT29 and HCT116 cells (Fig. 4C). WYE-132 treatment for 24 h also substantially reduced

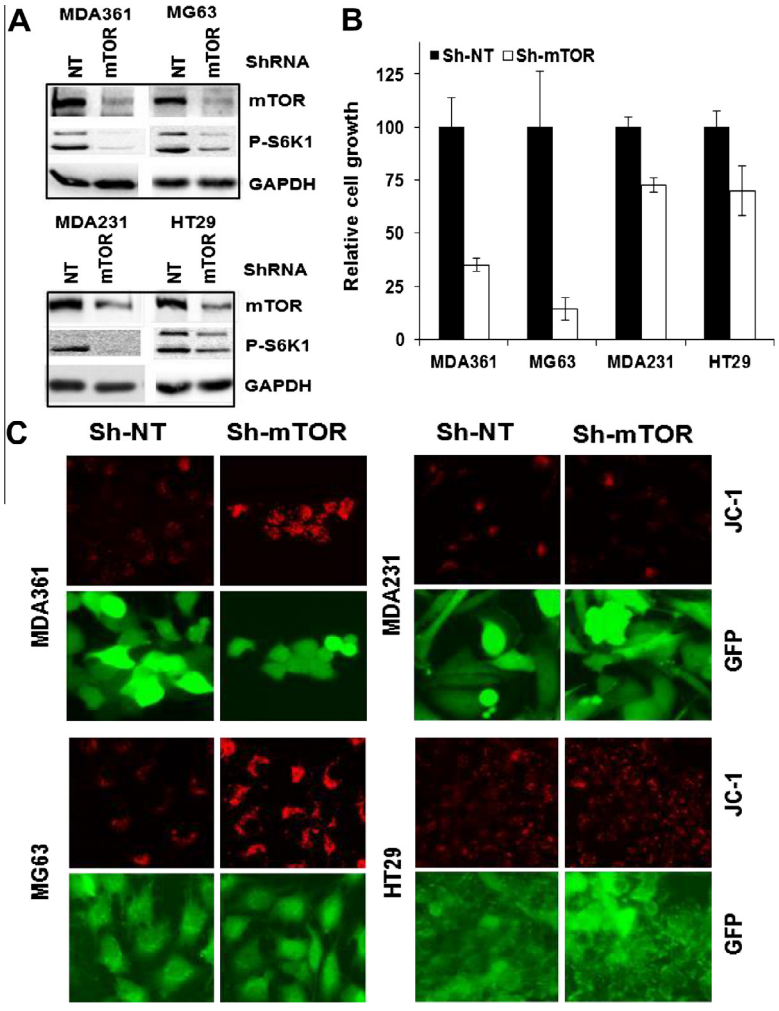

Fig. 3. mTOR-depletion elicits an increased mitochondrial $\Delta\psi_m$ in the mTOR-KI-sensitive cells. MDA361, MG63, HT29 and HCT116 cells were infected with GIPZ-Sh lentivirus corresponding to non-targeting (Sh-NT) or mTOR-targeting (Sh-mTOR). Puromycin-resistant cells (GFP positive) were plated in 12-well plates then subjected to immunoblotting (A) and cell growth measurement 4–6 days later via counting GFP-positive cells (B). (C) Cells similarly plated as in (A) were stained with JC-1 and subjected to JC-1 and GFP fluorescent images.

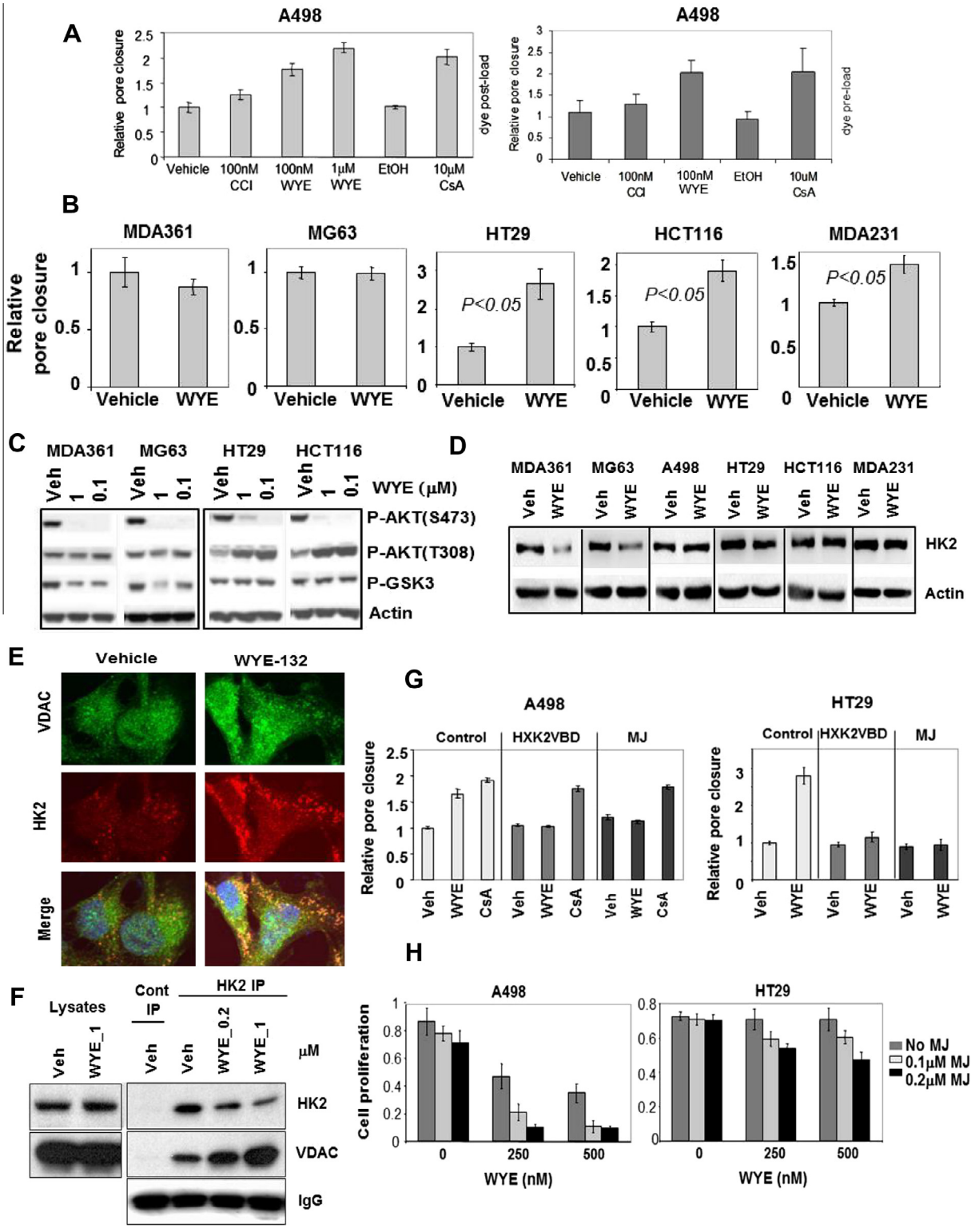

Fig. 4. The mTOR-KI-provoked mPTP closure reflects cellular resistance to mTOR-targeting and involves an enhanced HK2-VDAC association. (A) Dye post-loading (left) and dye pre-loading (right) mPTP permeability assays of A498 cells after treatment for 1 h with the indicated inhibitors. Pore permeability was assessed with fluorescent plate reading. (B) MDA361, MG63, HT29, HCT116 and MDA231 cells were treated with vehicle or 1 μM WYE-132 for 1 h then subjected to mPTP permeability measurements similarly as in (A). (C and D) Cells of MDA361, MG63, HT29, HCT116 and A498 were plated in 6-well plates, treated with the indicated inhibitors for 24 h then subjected to immunoblotting. (E) A498 cells were treated with either vehicle or 1 μM WYE-132 for 4 h, double-stained with VDAC and HK2 antibody and analyzed by confocal microscopy. (F) A498 cells were treated with vehicle, 0.2 or 1 μM or WYE-132 for 1 h followed by immunoprecipitation as described in Section 2. The immunocomplex was analyzed by immunoblotting. (G) A498 and HT29 cells were pretreated without or with 100 μM HXK2VBD or 400 nM MJ for 1 h, followed by treatment with vehicle, 1 μM WYE-132 (WYE) or 10 μM CsA for additional 1 h. The treated cells were subjected to mPTP assay similarly as in (B). (H) A498 and HT29 cells were treated with 0, 250 nM, 500 nM WYE-132 alone or in combination with the indicated doses of MJ for 3 days prior to cell growth assays.

HK2 expression in MDA361 and MG63 cells but not in A498, HT29 and HCT116 cells that displayed a reduced mPTP permeability (Fig. 4D). These results indicate that the mTOR-KI-provoked mPTP closure reflects cellular resistance to mTOR-targeting, which likely involves a feedback reactivation of AKT signaling, persistent inactivation of GSK3β and persistent HK2 expression in resistant cells.

Since mPTP permeability largely depends on VDAC, a main constitute of mPTP and its conductance is reduced via HK2 binding, we studied whether HK2-VDAC interaction may change after mTOR-inhibition. We chose A498 for these studies for its technical feasibility. Upon WYE-132 treatment, VDAC foci became highly prominent, which were predominantly co-localized with adenine nucleotide translocase 1, an inner membrane component of mPTP (not shown). Because it is well documented that HK2 binds to mitochondria through its interaction with VDAC [12,22,23], we examined the HK2-VDAC association by co-immunostaining. HK2 occasionally formed dot-like structure and a part of dots co-localized to VDAC foci. Upon WYE-132 treatment, formation of the HK2 dot-like structures became highly pronounced and majority of these structures co-localized to the VDAC foci (Fig. 4E). In co-immunoprecipitation assays, protein lysates from WYE-132-treated cells exhibited a significantly enhanced co-precipitation of VDAC with HK2 compared to that of vehicle-treated cells (Fig. 4F). We conclude from these results that mTOR-inhibition induces an increased recruitment of HK2 to VDAC in mitochondria, which is molecularly linked to the mPTP closure in mTOR-KI-resistant cells. To further examine the functional relevance of these findings, we analyzed the effects of an HK2-displacing peptide HXK2VBD and a natural product compound methyl jasmonate (MJ), both of which are known to block HK2-VADC association [22,23]. Pre-incubation of A498 or HT29 cells with either HXK2VBD or MJ completely blocked the WYE-132 effect on mPTP closure (Fig. 4G). As expected, HXK2VBD and MJ did not block the CsA-induced mPTP closure as CsA targets CyP-D independently from HK2-VDAC (Fig. 4G). Because the mPTP closure was most prominent in resistant cells, we tested whether MJ may enhance WYE-132's growth-inhibition in these cells. In both A498 and HT29 cells, while low nanomolar concentrations of MJ alone showed a moderate reduction in cell proliferation, it potentiated anti-proliferative activity of WYE-132, with up to 80% inhibition of A498 cell growth (Fig. 4H). Interestingly, MJ did not enhance WYE-132-drug sensitivity in cells that did not show prominent mPTP closure response (not shown). Collectively, the results in Fig. 4 indicate that the enhanced association of HK2-VDAC is mechanistically linked to the WYE-132-provoked mPTP reduction and the differential modulation of mPTP status by WYE-132 in various cancer cells contributes to therapeutic resistance to mTOR inhibition.

4. Discussion

Although rapalogs are already used clinically for several cancer types, their efficacy may be limited due to incomplete suppression of mTOR. Accordingly, new generation of mTOR kinase inhibitors have entered patient trials. To facilitate these efforts, it is not only necessary to investigate the new, rapalog-resistant mechanisms of mTOR but also critical to identify cancer types and underlying response biomarkers that will most benefit from mTOR-targeted treatments. The questions are raised as to how mTOR regulates mitochondrial dynamics in different cancer types under complex tumor signaling pathways and whether mitochondrial response plays a role in therapeutic outcome of mTOR-targeted therapy.

We have demonstrated that the global targeting of mTOR resulted in a profound increase of mΔψ. This effect was specific to mTOR-targeting as it was not observed in the same cells inhibited for the MEK/ERK pathway. The increase in mΔψ was highly evident in a subset of histologically diverse cancer cells that were most-sensitive to growth inhibition by WYE-132 and other selective mTOR-KIs such as AZD8055. In the most-sensitive cells, 1 μM CCI-779 also induced a moderate but significant increase of mΔψ (not shown). This result is in line with a previous report showing that rapamycin-treatment leads to an increased mΔψ in MCF7 cells, which correlates with autophagy and decreased cell survival [24]. Additionally, we found that inhibition of ALK oncogenic signaling in EML4-ALK oncogene-driven H2228 lung cancer cells by crizotinib leads to a dramatic increase in JC-1 fluorescence, to a level comparable to that by AZD8055 [25]. While further studies are required to delineate biochemical mechanism underlying this important mitochondrial response to mTOR-inhibition, a recent study showed that GSK3β inhibitors decreased mΔψ in HepG2 cells [26]. In our studies, mTOR-KIs caused dephosphorylation (activation) of GSK3β in the sensitive cells paralleling the increase of mΔψ, which was minimally observed in the most-resistant cells. It is thought that the prolonged hyperpolarization of mitochondria is detrimental and likely explains the exquisite growth inhibition sensitivity of these cells in response to mTOR-KI treatment. mTOR-KIs also provoked a decrease in mPTP permeability, a mitochondrial response known to promote survival [16,19,20]. Interestingly, this survival response was most prominently observed in the mTOR-KI-resistant cells and was not evident in cells that are highly susceptible to mTOR-KI growth suppression. Although the precise mechanism for the differential mPTP response in cancer cells remain to be elucidated, previous studies have established that AKT positively regulates HK2-VDAC association favoring mPTP closure [12,18,19] and that growth factor and/or inactivating phosphorylation of GSK3β could inhibit mPTP opening [20,21]. We have observed that the mTOR-KI-provoked mPTP closure in HT29 and HCT116 cells was accompanied by an increase in P-AKT(T308), persistent AKT-HK2 signaling and persistent phosphorylation (inactivation) of GSK3β. In contrast, mTOR-KI-treated MDA361 and MG63 cells displayed no such increase in P-AKT(T308) and demonstrated a substantial loss of HK2 expression and a decrease in GSK3β phosphorylation leading to an increased GSK3β activity. These cells elicited either mPTP opening (MDA361) or no change (MG63). These results are therefore consistent with the earlier proposal that mitochondrial permeability is subject to dynamic regulation in part through phosphorylation cascades.

The mTOR-KI-provoked mPTP closure was due, at least in part, to an enhanced interaction between HK2 and VDAC, a protective mechanism known to promote mitochondrial integrity and cell survival. Dissociation of HK2 from VDAC by an HK2-displacing peptide or an HK2-VADC disrupting compound MJ in the resistant cells completely blocked the effect of mTOR-KI on mPTP closure and enhanced growth suppression sensitivity to mTOR-KI. Our data therefore support a functional relationship among mTOR-KI-provoked mPTP closure, an enhanced HK2-VDAC association with cellular resistance.

The finding that the mTOR-KI-provoked mitochondrial alterations were differentially manifested in various cancer cells is relevant for mTOR inhibitor therapy. Several cell lines expressing hyperactive PI3K/AKT/mTOR activity status and/or growth factor-dependence, including those of LNCap, MDA361, MG63 and additional lines, generally elicited a profound increase in mΔψ yet minimal decrease in mPTP permeability in response to mTOR-KIs, whereas other cell lines carrying oncogenic K-Ras and/or B-Raf, including those of HCT116, MDA231 and HT29, all displayed the opposite effects. It is therefore likely that these common cancer signaling pathways can directly or indirectly influence mitochondrial homeostasis and metabolic properties that might be functionally linked to cellular susceptibility to mTOR inhibition. Our results also point to the complexity of differential reactivation of AKT survival pathway after mTOR-KI treatment, which likely contribute to therapeutic outcome.

Acknowledgments

The authors thank Lourdes Toral-Barza, Jun Xu, Boris Shor for technical assistance. This work was supported by Fudan University project #EZF301002 (K.Y.), National Natural Science Foundation of China project #81373442 (K.Y.) and by Wyeth/Pfizer.

References

[1] X.M. Ma, J. Blenis, Molecular mechanisms of mTOR-mediated translational control, Nat. Rev. Mol. Cell Biol. 10 (2009) 307–318.
[2] P. Polak, M.N. Hall, MTOR and the control of whole body metabolism, Curr. Opin. Cell Biol. 21 (2009) 209–218.
[3] I.J. Sipula, N.F. Brown, G. Perdomo, Rapamycin-mediated inhibition of mammalian target of rapamycin in skeletal muscle cells reduces glucose utilization and increases fatty acid oxidation, Metabolism 55 (2006) 1637–1644.
[4] J.T. Cunningham, J.T. Rodgers, D.H. Arlow, et al., MTOR controls mitochondrial oxidative function through a YY1-PGC-1alpha transcriptional complex, Nature 450 (2007) 736–740.
[5] S.M. Schieke, D. Phillips, J.P. McCoy, et al., The mammalian target of rapamycin (mTOR) pathway regulates mitochondrial oxygen consumption and oxidative capacity, J. Biol. Chem. 281 (2006) 27643–27652.
[6] S.M. Schieke, J.P. McCoy, T. Finkel, Coordination of mitochondrial bioenergetics with G1 phase cell cycle progression, Cell Cycle 7 (2008) 1782–1787.
[7] S.M. Schieke, M. Ma, L. Cao, et al., Mitochondrial metabolism modulates differentiation and teratoma formation capacity in mouse embryonic stem cells, J. Biol. Chem. 283 (2008) 28506–28512.
[8] B.N. Desai, B.R. Myers, S.L. Schreiber, FKBP12-rapamycin-associated protein associates with mitochondria and senses osmotic stress via mitochondrial dysfunction, Proc. Natl. Acad. Sci. U S A 99 (2002) 4319–4324.
[9] C. Betz, D. Stracka, C. Prescianotto-Baschong, et al., MTOR complex 2-Akt signaling at mitochondria-associated endoplasmic reticulum membranes (MAM) regulates mitochondrial physiology, Proc. Natl. Acad. Sci. U S A 110 (2013) 12526–12534.
[10] M. Colombi, K.D. Molle, D. Benjamin, et al., Genome-wide shRNA screen reveals increased mitochondrial dependence upon mTORC2 addiction, Oncogene 30 (2011) 1551–1565.
[11] A. Ramanathan, S.L. Schreiber, Direct control of mitochondrial function by mTOR, Proc. Natl. Acad. Sci. U S A 106 (2009) 22229–22232.
[12] S.P. Mathupala, Y.H. Ko, P.L. Pedersen, Hexokinase-2 bound to mitochondria: cancer's stygian link to the "Warburg Effect" and a pivotal target for effective therapy, Semin. Cancer Biol. 19 (2009) 17–24.
[13] K. Yu, C. Shi, L. Toral-Barza, et al., Beyond rapalog therapy: preclinical pharmacology and antitumor activity of WYE-125132, an ATP-competitive and specific inhibitor of mTORC1 and mTORC2, Cancer Res. 70 (2010) 621–631.
[14] B. Shor, J.J. Gibbons, R.T. Abraham, et al., Targeting mTOR globally in cancer: thinking beyond rapamycin, Cell Cycle 8 (2009) 3831–3837.
[15] V. Petronilli, G. Miotto, M. Canton, et al., Transient and long-lasting openings of the mitochondrial permeability transition pore can be monitored directly in intact cells by changes in mitochondrial calcein fluorescence, Biophys. J. 76 (1999) 725–734.
[16] D.H. Suh, M.K. Kim, H.S. Kim, et al., Mitochondrial permeability transition pore as a selective target for anti-cancer therapy, Front. Oncol. 3 (2013) 41.
[17] M. Crompton, H. Ellinger, A. Costi, Inhibition by cyclosporin A of a Ca^{2+}-dependent pore in heart mitochondria activated by inorganic phosphate and oxidative stress, Biochem. J. 255 (1988) 357–360.
[18] N. Majewski, V. Nogueira, P. Bhaskar, et al., Hexokinase–mitochondria interaction mediated by Akt is required to inhibit apoptosis in the presence or absence of Bax and Bak, Mol. Cell 16 (2004) 819–830.
[19] H. Azoulay-Zohar, A. Israelson, S. Abu-Hamad, et al., In self-defence: hexokinase promotes voltage-dependent anion channel closure and prevents mitochondria-mediated apoptotic cell death, Biochem. J. 377 (2004) 347–355.
[20] M. Juhaszova, D.B. Zorov, S.H. Kim, et al., Glycogen synthase kinase-3beta mediates convergence of protection signaling to inhibit the mitochondrial permeability transition pore, J. Clin. Invest. 113 (2004) 1535–1549.
[21] S. Das, R. Wong, N. Rajapakse, et al., Glycogen synthase kinase 3 inhibition slows mitochondrial adenine nucleotide transport and regulates voltage-dependent anion channel phosphorylation, Circ. Res. 103 (2008) 83–91.
[22] L. Galluzzi, O. Kepp, N. Tajeddine, et al., Disruption of the hexokinase–VDAC complex for tumor therapy, Oncogene 27 (2008) 4633–4635.
[23] N. Goldin, L. Arzoine, A. Heyfets, et al., Methyl jasmonate binds to and detaches mitochondria-bound hexokinase, Oncogene 27 (2008) 4636–4643.
[24] S. Paglin, N.Y. Lee, C. Nakar, et al., Rapamycin-sensitive pathway regulates mitochondrial membrane potential, autophagy, and survival in irradiated MCF-7 cells, Cancer Res. 65 (2005) 11061–11070.
[25] L. Meng, M. Shu, Y. Chen, et al., A novel lead compound CM-118: antitumor activity and new insight into the molecular mechanism and combination therapy strategy in c-Met- and ALK-dependent cancers, Cancer Biol. Ther. 15 (6) (2014) [Epub ahead of print].
[26] E.N. Maldonado, J. Patnaik, M.R. Mullins, et al., Free tubulin modulates mitochondrial membrane potential in cancer cells, Cancer Res. 70 (2010) 10192–10201.